IEEE Access
Multidisciplinary | Rapid Review | Open Access Journal

Received March 20, 2019, accepted April 29, 2019, date of publication May 9, 2019, date of current version May 23, 2019.

Digital Object Identifier 10.1109/ACCESS.2019.2915999

An Antiswing Trajectory Planning Method With State Constraints for 4-DOF Tower Cranes: Design and Experiments

ZHUOQING LIU, TONG YANG, NING SUN, (Member, IEEE), AND YONGCHUN FANG, (Senior Member, IEEE)

Institute of Robotics and Automatic Information Systems, College of Artificial Intelligence, Nankai University, Tianjin 300350, China
Tianjin Key Laboratory of Intelligent Robotics, Nankai University, Tianjin 300350, China

Corresponding author: Ning Sun (sunn@nankai.edu.cn)

This work was supported in part by the National Natural Science Foundation of China under Grant 61873134 and Grant U1706228, in part by the Self-Developed Experimental Teaching Instrument/Equipment Project of Nankai University under Grant 2018nkzzyq15, and in part by the Fundamental Research Funds for the Central Universities under Grant 63191718.

ABSTRACT As a kind of indispensable equipment widely applied in construction sites, tower crane systems have complicated nonlinear dynamical characteristics, which make controller design challenges. Apart from the primary control objective of accurate slew/translation positioning and effective swing elimination, another important task is to ensure the satisfactory state transient performance, and simultaneously, the transportation time also needs to be as short as possible. To solve the above issues, in this paper, a new time-(sub)optimal trajectory planning method is proposed, which is the first solution to generate antiswing trajectories for four-degree of freedom (DOF) tower crane systems with state constraints. In particular, three auxiliary signals are constructed, and the reference trajectories for the jib slew and trolley translation can be obtained by the elaborately designed trajectories related to auxiliary signals. Hence, based on the reference trajectories for the jib/trolley, the payload can be driven to the desired location accurately with rapid payload swing elimination; moreover, the state variables, payload displacement, and their velocities are all restricted within the specific ranges. Finally, a series of hardware experiments are implemented to verify the effectiveness of the proposed method.

INDEX TERMS Tower cranes, underactuated systems, trajectory planning, vibration/swing suppression.

I. INTRODUCTION

With the development of modern industry, cranes, as indispensable transportation equipment in many fields, play increasingly important roles in practice. According to their different dynamical characteristics, cranes can be classified into many types, such as tower cranes [1], overhead cranes [2]–[4], boom cranes [5]–[7], offshore container cranes [8]–[11] and so on. Although different cranes have different mechanical structures and application fields, a common feature is that they have fewer independent actuators than the degrees of freedom (DOFs) of systems. Hence, cranes are a kind of typical underactuated systems.

Compared with fully-actuated systems, underactuated systems are superior in energy saving, cost reduction, weight reduction, and system flexibility; however, they are more difficult to control due to the lack of control inputs. Hence, the studies of various underactuated systems have become a hot topic in recent decades [12]–[27]. In particular, many researchers concentrate on the control problems of crane systems, and the proposed methods can be roughly divided into open loop control and closed loop control. When the working environment is without serious disturbances, open loop control methods are effective, including input shaping methods [28], [29] and trajectory planning methods [30]–[33]. However, when the external disturbances cannot be ignored, to further improve the robustness of systems, some closed loop methods are proposed, such as delayed reference noncolocated control [34], sliding mode control [35], [36], nonlinear control [37]–[41], adaptive control [42], [43], intelligent control [44]–[49], etc.

When putting up high buildings in construction sites, tower cranes have irreplaceable advantages compared with other

The associate editor coordinating the review of this manuscript and approving it for publication was Chuxiong Hu.

crane systems. With increasingly widespread applications of tower cranes, the safety issues of them attract extensive attention. Nowadays, almost all tower cranes still rely on manual operations, which not only require experienced operators, but also cannot guarantee the accurate positioning or high efficiency. Furthermore, manual manipulations have significant potential risks, and a slight mistake may lead to serious accidents and irreparable losses. As a result, it is urgent and essential to design control methods for tower cranes to realize accurate positioning and effective swing elimination.

Compared with overhead cranes, the complicated slew motions generate additional inertial forces and centrifugal forces in tower crane systems; moreover, the state coupling is enhanced due to the complex nonlinear dynamical characteristics of tower cranes. Hence, it is more difficult to accomplish the control task (i.e., accurate positioning and swing elimination). To solve the aforementioned problems, lots of efforts have been made currently. In [50], to simplify the complicated dynamics of tower cranes, Ju *et al.* use the finite element method to linearize the model and analyze the dynamical response thoroughly. In [51], scheduling feedback control methods are developed to realize payload swing suppression for tower cranes. A series of input shaping control approaches are applied to reduce the payload swing by shaping the desired inputs based on the system natural frequency in [52], [53]. In [54], a model predictive control method is proposed to realize path following. In [55], Sun *et al.* develop an adaptive nonlinear control method according to the complicated dynamics of tower cranes, which can reduce unexpected overshoots for the slew and translation motion. Further, a robust adaptive technique is applied to tower cranes in [56]. In [1], to reduce the steady errors, an integral term is introduced into the nonlinear controller and the control performance is further improved. In addition, some intelligence-based control methods are presented, including neural network-based control [57], [58] and fuzzy-based control [59].

Although existing control approaches have made some progresses, few of them can completely guarantee the transient performance of the state variables. From the practical perspective, to ensure the control inputs to be constrained within the hardware limits, the velocities and accelerations of the trolley and jib need to be restricted within reasonable ranges. In addition, the payload swing angles and their velocities should also satisfy the specified physical constraints, so that tower cranes can realize smooth transportation to avoid safety accidents. Therefore, apart from the primary control objective, the above physical constraints are expected to be satisfied simultaneously; moreover, to ensure the work efficiency of tower cranes, the transportation time is expected to be short enough, which undoubtedly increases the difficulty of controller design. Unfortunately, few existing methods can theoretically guarantee the state variables to be restricted within physical constraints during the shortest possible transportation time.

In this paper, we present a new trajectory planning method for 4-DOF tower crane systems, which can drive the jib and trolley to the desired positions accurately with payload swing elimination. Moreover, the physical constraints of the state variables and their velocities are all satisfied in the entire transportation process. Finally, the effectiveness and reliability of the proposed method are verified by some hardware experiments implemented on a self-built testbed. The merits of this paper are listed below.

- In the process of trajectory planning for the auxiliary signals, some practical constraints (including the jib slew angular velocity and acceleration, trolley translation velocity and acceleration, swing angles, swing angular velocities, and payload position velocities) are fully taken into consideration. Furthermore, a optimization problem is formulated and solved to ensure the transportation time is as short as possible on the premise of meeting the constraints. Hence, during the entire transportation, apart from accurate positioning and effective payload swing elimination, the satisfactory transient performance of the state variables and payload position can be ensured while guaranteeing time (sub)optimality.
- Two groups of hardware experiments are implemented on the self-built tower crane platform. By some comparative experiments and different working conditions, the effectiveness of the proposed method are validated.

The remaining parts of this paper are organized as follows. In Section II, we introduce the underactuated tower crane system dynamics and formulate the problem, which describes the control task mathematically. Then, the entire trajectory planning process is implemented in Section III, including auxiliary signals construction, trajectory parameterizations, and the solution of the optimization problem. In Section IV, some experiments are implemented to verify the effectiveness of the proposed method. Finally, Section V gives the conclusion of this paper.

II. PROBLEM FORMULATION

A. TOWER CRANE DYNAMICS

The underactuated 4-DOF tower crane system in the inertia frame *O-XYZ* is shown in FIGURE 1, whose dynamical equations are as follows:

$$\begin{aligned}
&\left[m\left(\theta_1^2+\theta_2^2\right)l^2+2msl\theta_1+J+(m+M)s^2\right]\ddot{\alpha}\\
&\quad-ml\theta_2\ddot{s}-ml^2\theta_2\ddot{\theta}_1+ml(s+l\theta_1)\ddot{\theta}_2\\
&\quad+2(m+M)s\dot{s}\dot{\alpha}+2mls\dot{\alpha}\dot{\theta}_1-ml\theta_2\left(2\dot{\alpha}\theta_1+\dot{\theta}_2\right)s\dot{\theta}_2\\
&\quad+2ml\theta_1\dot{s}\dot{\alpha}+2ml^2\theta_1\dot{\alpha}\dot{\theta}_1+ml^2\theta_1\theta_2\dot{\theta}_1^2\\
&\quad+2ml^2\theta_2\dot{\alpha}\dot{\theta}_2+2ml^2\theta_2^2\dot{\theta}_1\dot{\theta}_2=u_1, \qquad (1)\\
&-ml\theta_2\ddot{\alpha}+(m+M)\ddot{s}+ml\ddot{\theta}_1-ml\theta_1\theta_2\ddot{\theta}_2\\
&\quad-(m+M)s\dot{\alpha}^2-2ml\theta_2\dot{\theta}_1\dot{\theta}_2\\
&\quad-ml\left[\theta_1\left(\dot{\alpha}^2+\dot{\theta}_1^2+\dot{\theta}_2^2\right)+2\dot{\alpha}\dot{\theta}_2\right]=u_2, \qquad (2)\\
&-ml^2\theta_2\ddot{\alpha}+ml\ddot{s}+ml^2\ddot{\theta}_1-ml(s+l\theta_1)\dot{\alpha}^2\\
&\quad-2ml^2\left(\dot{\alpha}+\dot{\theta}_1\theta_2\right)\dot{\theta}_2+mgl\theta_1=0, \qquad (3)
\end{aligned}$$

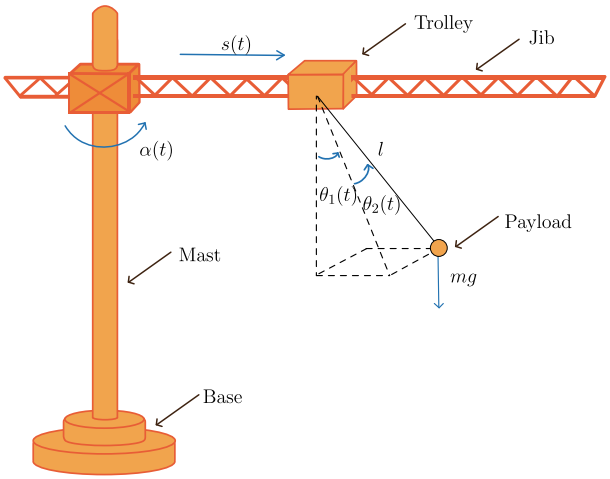

FIGURE 1. Model of a 4-DOF tower crane system.

$$
\begin{aligned}
&ml\left(s+l\theta_1\right)\ddot{\alpha}-ml\theta_1\theta_2\ddot{s}+ml^2\ddot{\theta}_2+2ml\dot{s}\dot{\alpha}\\
&+ml\left(s\theta_1\theta_2-l\theta_2\right)\dot{\alpha}^2\\
&+2ml^2\dot{\alpha}\dot{\theta}_1+ml^2\dot{\theta}_1^2\theta_2+mgl\theta_2=0,
\end{aligned}
\tag{4}
$$

where α represents the jib slew angle, s stands for the trolley translation displacement, the payload swing is described by θ_1 and θ_2 as shown in FIGURE 1, J is the moment of inertia of the jib, l denotes the suspension rope length, M and m represent the trolley mass and the payload mass, respectively, g is the gravity constant, and u_1, u_2 denote the slew control toque and the translation control force, respectively.

B. PROBLEM STATEMENT

The control objective of tower crane systems is to drive the payload toward the desired location fast and accurately with effective payload swing suppression. Moreover, to ensure the satisfactory transient performance, the state variables of tower crane systems should be restricted within suitable ranges. Hence, the entire control task can be divided into four subtasks as follows:

1) The trolley and jib need to arrive at the desired positions s_r, α_r from the initial positions s_{r0}, α_{r0}, respectively, during the transportation time T, while both swing angles θ_1, θ_2 should be zero after T. Meanwhile, the trolley velocity and acceleration, the jib angular velocity and angular acceleration, and the swing angular velocities should all become zero at T, i.e.,

$$
\begin{aligned}
s(0)&=s_{r0}, \quad \dot{s}(0)=0, \ \ddot{s}(0)=0,\\
s(T)&=s_r, \quad \dot{s}(T)=0, \quad \ddot{s}(T)=0,\\
\alpha(0)&=\alpha_{r0}, \quad \dot{\alpha}(0)=0, \ \ddot{\alpha}(0)=0,\\
\alpha(T)&=\alpha_r, \quad \dot{\alpha}(0)=0, \ \ddot{\alpha}(0)=0,\\
\theta_1(0)&=\theta_2(0)=0, \quad \dot{\theta}_1(0)=\dot{\theta}_2(0)=0,\\
\theta_1(T)&=\theta_2(T)=0, \quad \dot{\theta}_1(T)=\dot{\theta}_2(T)=0.
\end{aligned}
\tag{5}
$$

2) To guarantee the control inputs to be restricted within the hardware limits, the trolley velocity and acceleration together with the jib angular velocity and angular acceleration should be appropriately constrained. Hence, the following relationships can be satisfied:

$$
|\dot{s}| \le v_{1\max}, \quad |\ddot{s}| \le a_{1\max}, \tag{6}
$$

$$
|\dot{\alpha}| \le v_{\alpha\max}, \quad |\ddot{\alpha}| \le a_{\alpha\max}, \tag{7}
$$

where $v_{1\max}$ and $a_{1\max}$ denote the velocity and acceleration constraints of the trolley, respectively, $v_{\alpha\max}$ and $a_{\alpha\max}$ represent the largest permitted amplitudes of the jib slew angular velocity and angular acceleration, respectively.

3) To ensure safety in real applications, the payload swing angles and their angular velocities should be within reasonable ranges, in the sense that,

$$
\begin{aligned}
&|\theta_1| \le \theta_{1\max}, \quad |\theta_2| \le \theta_{2\max},\\
&|\dot{\theta}_1| \le v_{\theta_{1\max}}, \quad |\dot{\theta}_2| \le v_{\theta_{2\max}},
\end{aligned}
\tag{8}
$$

where $\theta_{1\max}$, $\theta_{2\max}$ denote the maximum allowable amplitudes of the payload swing angles, respectively, $v_{\theta_{1\max}}$, $v_{\theta_{2\max}}$ represent the permitted upper bounds of the payload swing angles velocities, respectively.

4) To increase the work efficiency of tower crane systems, the transportation time T is expected to be as short as possible.

By taking the above-mentioned constraints into consideration, we can summarize the following optimization problem, which will be further discussed in the next section:

$$
\text{minimize } T, \quad \text{subject to (5)-(8).} \tag{9}
$$

III. TRAJECTORY PLANNING WITH STATE CONSTRAINTS

In this section, we first analyze the dynamics of tower crane systems and accordingly construct a group of auxiliary signals, which can describe the trolley displacement and payload position. Then, the optimization problem formulated in (9) is constructed and several trigonometric trajectories with state constraints are designed for the auxiliary signals. According to the relationships between the auxiliary signals and the state variables, the reference trajectories for the trolley and jib can be derived.

A. AUXILIARY SIGNALS CONSTRUCTION

The top view of the tower crane model is shown as FIGURE 2. A coordinate system is established, which regards O as the original point. Then, we can obtain the following payload position in the direction of X axis and Y axis, respectively:

$$
x = s\cos\alpha + l\theta_1\cos\alpha - l\theta_2\sin\alpha, \tag{10}
$$

$$
y = s\sin\alpha + l\theta_1\sin\alpha + l\theta_2\cos\alpha. \tag{11}
$$

Then, combining (10) and (11) yields

$$
\begin{aligned}
\theta_1 &= \frac{1}{l}\left(x\cos\alpha + y\sin\alpha - s\right),\\
\theta_2 &= \frac{1}{l}\left(y\cos\alpha - x\sin\alpha\right).
\end{aligned}
\tag{12}
$$

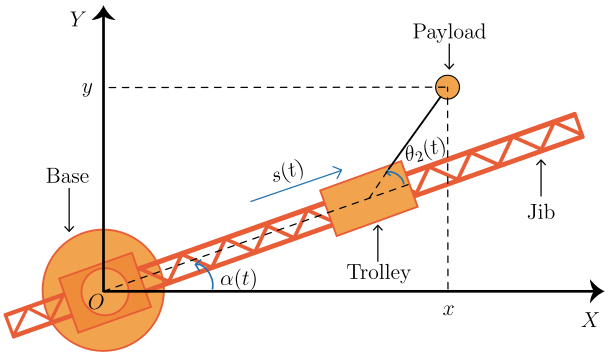

FIGURE 2. The top view of the tower crane model.

Moreover, the second derivatives of x and y can be expressed as

$$\begin{aligned}\ddot{x} = {} & \ddot{s}\cos\alpha - 2\dot{s}\dot{\alpha}\sin\alpha - s\dot{\alpha}^2\cos\alpha - s\ddot{\alpha}\sin\alpha \\ & + l\ddot{\theta}_1\cos\alpha - l\ddot{\theta}_2\sin\alpha - 2l\dot{\theta}_1\dot{\alpha}\sin\alpha \\ & - 2l\dot{\theta}_2\dot{\alpha}\cos\alpha - l\theta_1\ddot{\alpha}\sin\alpha - l\theta_1\dot{\alpha}^2\cos\alpha \\ & - l\theta_2\ddot{\alpha}\cos\alpha + l\theta_2\dot{\alpha}^2\sin\alpha, \qquad (13) \\ \ddot{y} = {} & \ddot{s}\sin\alpha + 2\dot{s}\dot{\alpha}\cos\alpha - s\dot{\alpha}^2\sin\alpha + s\ddot{\alpha}\cos\alpha \\ & + l\ddot{\theta}_1\sin\alpha + l\ddot{\theta}_2\cos\alpha + 2l\dot{\theta}_1\dot{\alpha}\cos\alpha \\ & - 2l\dot{\theta}_2\dot{\alpha}\sin\alpha + l\theta_1\ddot{\alpha}\cos\alpha - l\theta_1\dot{\alpha}^2\sin\alpha \\ & - l\theta_2\ddot{\alpha}\sin\alpha - l\theta_2\dot{\alpha}^2\cos\alpha. \qquad (14)\end{aligned}$$

By some complex calculations, (13) and (14) can be rearranged as

$$\begin{aligned}\ddot{x}\cos\alpha + \ddot{y}\sin\alpha = {} & \ddot{s} - s\dot{\alpha}^2 + l\ddot{\theta}_1 - 2l\dot{\theta}_2\dot{\alpha} - l\theta_1\dot{\alpha}^2 \\ & - l\theta_2\ddot{\alpha}, \\ \ddot{x}\sin\alpha - \ddot{y}\cos\alpha = {} & -2\dot{s}\dot{\alpha} - s\ddot{\alpha} - l\ddot{\theta}_2 - 2l\dot{\theta}_1\dot{\alpha} - l\theta_1\ddot{\alpha} \\ & + l\theta_2\dot{\alpha}^2. \qquad (15)\end{aligned}$$

Then, on the basis of (3), (4), and (15), we can obtain the following equations:

$$\ddot{x}\cos\alpha + \ddot{y}\sin\alpha = -g\theta_1, \qquad (16)$$

$$\ddot{x}\sin\alpha - \ddot{y}\cos\alpha = g\theta_2. \qquad (17)$$

Next, we multiply (16) and (17) by $\cos\alpha$ and $\sin\alpha$, respectively as

$$\begin{aligned}\ddot{x}\cos\alpha^2 + \ddot{x}\sin\alpha^2 = {} & \frac{g}{l}(-\theta_1 + \theta_2) \\ \Longrightarrow \alpha = {} & \arccos\frac{\frac{l}{g}\ddot{x} + x}{s}, \qquad (18)\end{aligned}$$

where (12) is used. Hence, by substituting (18) into (12), θ_1 and θ_2 can be expressed as follows:

$$\begin{aligned}\theta_1 = {} & \frac{1}{l}\left[\frac{x\left(\frac{l}{g}\ddot{x} + x\right)}{s} + y\sin\left(\arccos\frac{\frac{l}{g}\ddot{x} + x}{s}\right) - s\right], \\ \theta_2 = {} & \frac{1}{l}\left[\frac{y\left(\frac{l}{g}\ddot{x} + x\right)}{s} - x\sin\left(\arccos\frac{\frac{l}{g}\ddot{x} + x}{s}\right)\right]. \qquad (19)\end{aligned}$$

From the foregoing analysis, we represent all state variables of tower crane systems as algebraic combinations of the auxiliary signals, i.e., x, y, s, and their derivatives, which can facilitate the trajectory planning process for the jib and trolley subsequently.

Then, by combining (5), (18), and (19), we can obtain the constraints of the auxiliary signals transformed from the state variables constraints, which can be expressed as follows:

$$\begin{aligned}& x(0) = x_{r0}, \quad x^{(k)}(0) = 0,\ x(T) = x_r,\ x^{(k)}(T) = 0, \\ & y(0) = y_{r0}, \quad y^{(k)}(0) = 0,\ y(T) = y_r,\ y^{(k)}(T) = 0, \\ & s(0) = s_{r0}, \quad s^{(p)}(0) = 0,\ s(T) = s_r,\ s^{(p)}(T) = 0, \\ & k = 1, 2, 3, 4, \quad p = 1, 2, 3, \qquad (20)\end{aligned}$$

where T is the transportation time, x_{r0}, y_{r0} represent the payload initial positions in the X-O-Y plane, x_r, y_r denote the payload desired positions, and s_{r0}, s_r are the initial position and desired position of the trolley, respectively.

In addition, with the auxiliary signals exactly describing the trolley displacement and payload position, their derivatives represent the velocities and accelerations of the trolley and payload, respectively. To ensure smooth transportation of tower crane systems, they should be restricted as well, in the sense that

$$\begin{aligned}|\dot{x}|,\ |\dot{y}| \le v_{i\max}, \quad & i = 2, 3, \\ |\ddot{x}|,\ |\ddot{y}| \le a_{i\max}, \quad & i = 2, 3, \\ |s^{(3)}|,\ |x^{(3)}|,\ |y^{(3)}| \le j_{i\max}, \quad & i = 1, 2, 3, \qquad (21)\end{aligned}$$

where $v_{i\max}$, $a_{i\max}$, $j_{i\max}$ denote the velocity, acceleration and jerk boundaries of the auxiliary signals s, x, and y, respectively.

B. TRIGONOMETRIC TRAJECTORY PARAMETERIZATIONS

To achieve the control objective, appropriate curves are needed to parameterize the auxiliary signals. For the position of payload x and y, noticing that there are 10 state constraints in (20), 5-order trigonometric spline curves with unknown parameters are chosen as follows [60]:

$$\begin{aligned}x^*(t) = {} & a_0(x_{r0} + x_r) + \sum_{k=1}^{4}(a_k\cos k\tau_1 + b_k\sin k\tau_1) \\ & \cdot (x_r - x_{r0}) + a_5\sin\left(5\tau_1 - \frac{5\pi}{4}\right)(x_r - x_{r0}), \\ y^*(t) = {} & m_0(y_r + y_{r0}) + \sum_{k=1}^{4}(m_k\cos k\tau_1 + n_k\sin k\tau_1) \\ & \cdot (y_r - y_{r0}) + m_5\sin\left(5\tau_1 - \frac{5\pi}{4}\right)(y_r - y_{r0}), \qquad (22)\end{aligned}$$

where $0 \le t \le T$, $\tau_1 = \pi t/2T$, a_0, a_k, b_k, m_0, m_k, and n_k are parameters to be determined. As for the trolley displacement s, we select the following 4-order trigonometric spline curve

similarly:

$$s^*(t) = p_0 (s_{r0} + s_r) + \sum_{k=1}^{3} (p_k \cos k\tau_2 + q_k \sin k\tau_2) \cdot (s_r - s_{r0}) + p_4 \sin(4\tau_2 - 2\pi)(s_r - s_{r0}), \quad (23)$$

where $\tau_2 = \pi t/T$, p_0, p_k, and q_k are parameters to be determined.

Then, combining (20), (22), and (23), we can derive three groups of linear equations related to $x^{(i)}$, $y^{(i)}$, and $s^{(i)}$, where $i = 0, 1, 2, 3, 4$. By solving these equations, we can calculate the parameters as follows:

$$\begin{aligned}
&a_0 = m_0 = \frac{1}{2}, \quad a_1 = m_1 = -\frac{125}{8}, \ a_2 = m_2 = \frac{55}{2}, \\
&a_3 = m_3 = -\frac{215}{16}, \quad a_4 = m_4 = 0, \ a_5 = m_5 = \frac{17\sqrt{2}}{16}, \\
&b_1 = n_1 = \frac{125}{8}, \quad b_2 = n_2 = 0, \ b_3 = n_3 = -\frac{215}{16}, \\
&b_4 = n_4 = \frac{15}{2}, \quad p_0 = \frac{1}{2}, \ p_1 = -\frac{9}{16}, \\
&p_3 = \frac{1}{16}, \quad p_2 = p_4 = q_1 = q_2 = q_3 = 0. \quad (24)
\end{aligned}$$

Thus, the transportation time T is the only parameter to be determined in the trajectories for the auxiliary signals. According to the constraints in (6) and (21), the derivatives of the auxiliary signals can be redescribed as

$$\begin{aligned}
&\dot{x}^*(t) = \frac{\pi}{2T}\frac{dx^*(\tau_1)}{d\tau_1}, \quad \ddot{x}^*(t) = \left(\frac{\pi}{2T}\right)^2 \frac{d^2x^*(\tau_1)}{d\tau_1^2}, \\
&x^{*(3)}(t) = \left(\frac{\pi}{2T}\right)^3 \frac{d^3x^*(\tau_1)}{d\tau_1^3}, \quad \dot{y}^*(t) = \frac{\pi}{2T}\frac{dy^*(\tau_1)}{d\tau_1}, \\
&\ddot{y}^*(t) = \left(\frac{\pi}{2T}\right)^2 \frac{d^2y^*(\tau_1)}{d\tau_1^2}, \quad y^{*(3)}(t) = \left(\frac{\pi}{2T}\right)^3 \frac{d^3y^*(\tau_1)}{d\tau_1^3}, \\
&\dot{s}^*(t) = \frac{\pi}{T}\frac{ds^*(\tau_2)}{d\tau_2}, \quad \ddot{s}^*(t) = \left(\frac{\pi}{T}\right)^2 \frac{d^2s^*(\tau_2)}{d\tau_2^2}, \\
&s^{*(3)}(t) = \left(\frac{\pi}{T}\right)^3 \frac{d^3s^*(\tau_2)}{d\tau_2^3}. \quad (25)
\end{aligned}$$

Hence, we can obtain the following equations:

$$\begin{aligned}
&\max_{t\in[0,T]} \left|x^{*(k)}(t)\right| = \left(\frac{\pi}{2T}\right)^k \max_{\tau_1\in[0,\frac{\pi}{2}]} \left|\frac{d^kx^*(\tau_1)}{d\tau_1^k}\right|, \\
&\max_{t\in[0,T]} \left|y^{*(k)}(t)\right| = \left(\frac{\pi}{2T}\right)^k \max_{\tau_1\in[0,\frac{\pi}{2}]} \left|\frac{d^ky^*(\tau_1)}{d\tau_1^k}\right|, \\
&\max_{t\in[0,T]} \left|s^{*(k)}(t)\right| = \left(\frac{\pi}{T}\right)^k \max_{\tau_2\in[0,\pi]} \left|\frac{d^ks^*(\tau_2)}{d\tau_2^k}\right|, \quad (26)
\end{aligned}$$

where $k = 1, 2, 3$. After defining the following parameters as:

$$\begin{aligned}
&\alpha_1 = \frac{\pi}{v_{1\max}}, \quad \alpha_2 = \frac{\pi^2}{a_{1\max}}, \ \alpha_3 = \frac{\pi^3}{j_{1\max}}, \\
&\beta_1 = \frac{\pi}{2v_{2\max}}, \quad \beta_2 = \frac{\pi^2}{4a_{2\max}}, \ \beta_3 = \frac{\pi^3}{8j_{2\max}}, \\
&\gamma_1 = \frac{\pi}{2v_{3\max}}, \quad \gamma_2 = \frac{\pi^2}{4a_{3\max}}, \ \gamma_3 = \frac{\pi^3}{8j_{3\max}},
\end{aligned}$$

we can obtain the lower bound of the transportation time T_l as

$$\begin{aligned}
T_l = \max\Bigg\{ &\left(\alpha_k \max\left|\frac{d^ks^*(\tau_2)}{d\tau_2^k}\right|\right)^{\frac{1}{k}}, \\
&\left(\beta_k \max\left|\frac{d^ky^*(\tau_1)}{d\tau_1^k}\right|\right)^{\frac{1}{k}}, \\
&\left(\gamma_k \max\left|\frac{d^kx^*(\tau_1)}{d\tau_1^k}\right|\right)^{\frac{1}{k}} \Bigg\}, \quad (27)
\end{aligned}$$

where $k = 1, 2, 3$. Thus, the optimization problem formulated in (9) can be redescribed as follows:

$$\text{minimize } T, \quad \text{subject to (7), (8), and (27)}, \quad (28)$$

whose solution is calculated in the next subsection.

C. OPTIMIZATION PROBLEM SOLUTION

As shown in Algorithm 1, to solve the optimization problem described in (28), a bisection method is presented. In Algorithm 1, we define $T_l, T_u \in R^+$ as the allowable minimum and maximum of the parameter T, respectively, and ϵ as the optimization admissible error, is employed to determine when to finish the optimization process.

Algorithm 1 Solving (28)

Input: $T_l, T_u, \theta_{1\max}, \theta_{2\max}, v_{\theta_{1\max}}, v_{\theta_{2\max}}, v_{\alpha\max}, a_{\alpha\max}$
Output: T^*
1: **while** $|T_u - T_l| > \epsilon$ **do**
2: set: $T_s = (T_l + T_u)/2$
3: **if** the constraints in (7) and (8) are all satisfied **then**
4: set $T_u = T_s$
5: **else**
6: set: $T_l = T_s$
7: **end if**
8: **end while**
9: set $T^* = T_s$

Accordingly, on the basis of (24) and the optimized transportation time T^*, we can respectively obtain the following trigonometric trajectories for the auxiliary signals x, y, and s:

$$x^*(t) = \begin{cases} \frac{1}{2}(x_{r0} + x_r) + (x_r - x_{r0}) \Big[-\frac{125}{8}\cos\tau_1 \\ +\frac{125}{8}\sin\tau_1 + \frac{55}{2}\cos 2\tau_1 - \frac{215}{16}\cos 3\tau_1 \\ -\frac{215}{16}\sin 3\tau_1 + \frac{15}{2}\sin 4\tau_1 \\ +\frac{17\sqrt{2}}{16}\sin\left(5\tau_1 - \frac{5\pi}{4}\right)\Big], \quad t \in [0, T^*] \\ x_r, \quad t > T^*, \end{cases} \quad (29)$$

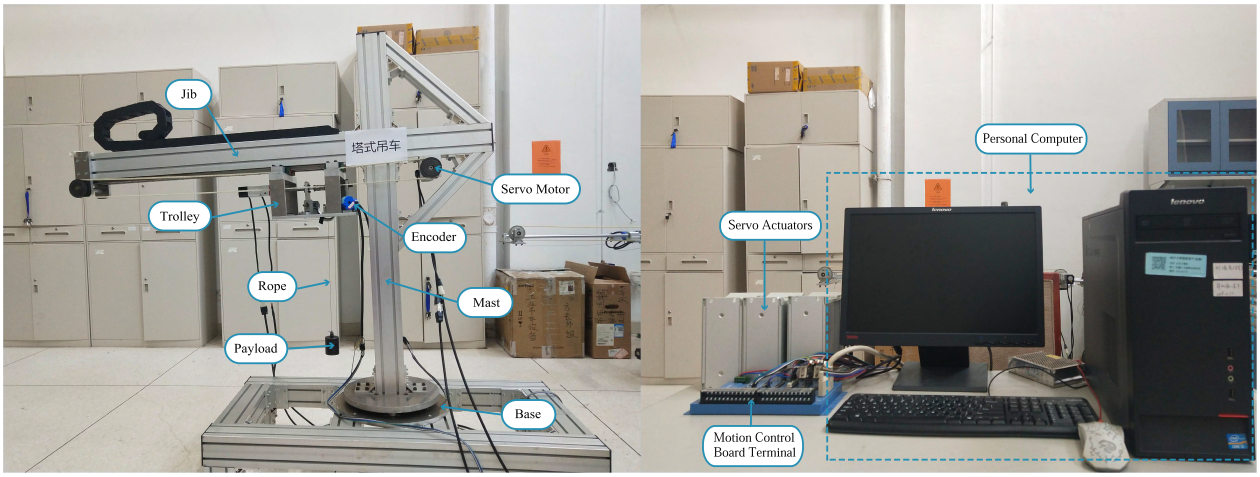

FIGURE 3. A self-built 4-DOF tower crane experimental testbed.

$$y^*(t) = \begin{cases} \frac{1}{2}(y_{r0}+y_r)+(y_r-y_{r0})\left[-\frac{125}{8}\cos\tau_1 \right. \\ +\frac{125}{8}\sin\tau_1+\frac{55}{2}\cos 2\tau_1-\frac{215}{16}\cos 3\tau_1 \\ -\frac{215}{16}\sin 3\tau_1+\frac{15}{2}\sin 4\tau_1 \\ \left.+\frac{17\sqrt{2}}{16}\sin\left(5\tau_1-\frac{5\pi}{4}\right)\right], \quad t\in[0,T^*] \\ y_r, \quad t>T^*, \end{cases} \tag{30}$$

$$s^*(t) = \begin{cases} \frac{1}{2}(s_{r0}+s_r)+(s_r-s_{r0})\left(-\frac{9}{16}\cos\tau_2 \right. \\ \left.+\frac{1}{16}\cos 3\tau_2\right), \quad t\in[0,T^*] \\ s_r, \quad t>T^*. \end{cases} \tag{31}$$

Consequently, according to (18) and (19), we can derive that

$$\begin{aligned} \alpha^* &= \arccos\frac{\frac{l}{g}\ddot{x}^*+x^*}{s^*}, \\ \theta_1^* &= \frac{1}{l}\left[\frac{x^*\left(\frac{l}{g}\ddot{x}^*+x^*\right)}{s^*}-s^* \right. \\ &\quad \left.+y^*\sin\left(\arccos\frac{\frac{l}{g}\ddot{x}^*+x^*}{s^*}\right)\right], \\ \theta_2^* &= \frac{1}{l}\left[\frac{y^*\left(\frac{l}{g}\ddot{x}^*+x^*\right)}{s^*}-x^*\sin\left(\arccos\frac{\frac{l}{g}\ddot{x}^*+x^*}{s^*}\right)\right]. \end{aligned} \tag{32}$$

Thus, we obtain the reference trajectories of all the state variables, which can suppress the payload swing effectively and simultaneously ensure the satisfactory transient performance during a shortest possible transportation time. To validate the actual performance, some hardware experiments are implemented in the next section.

IV. HARDWARE EXPERIMENTS

To testify the effectiveness and reliability of the proposed method, two groups of hardware experiments are implemented in this section. We first describe the tower crane experimental testbed, and then give the experimental results and analysis.

A. TOWER CRANE EXPERIMENTAL TESTBED

As shown in FIGURE 3, the tower crane experimental testbed is composed of the mechanism, driving devices with sensors, and the computer control system.

The jib slew and trolley translation motions are actuated by two AC servo motors. Utilizing the encoders equipped in the AC servo motors, the slew angle and translation displacement can be measured. In addition, a rope connects the payload to the trolley. To obtain the payload motion in real-time, angular encoders are installed beneath the trolley. The system parameters of the self-built tower crane testbed are set as $M = 7$ kg, $J = 6.8$ kg·m, and $g = 9.8$ kg/m^2.

Regarding the computer control system, a motion control board is utilized to collect/convey sensor signals and generate control commands. In addition, the MATLAB/Simulink running in Windows XP is used to calculate control commands to implement real-time control with the sample time set as 5 ms.

B. EXPERIMENTAL RESULTS AND ANALYSIS

In Experiment 1, we compare the proposed method with the linear quadratic regulator (LQR) method. In Experiment 2, the payload mass is changed in Case 1 to validate the robustness against the changes of payload mass; in Case 2, to verify the effectiveness of the proposed method under different working requirements, the rope length and desired positions are changed simultaneously.

1) EXPERIMENT 1

The experimental parameters, including the payload mass, rope length, initial/desired positions of the jib and trolley, and

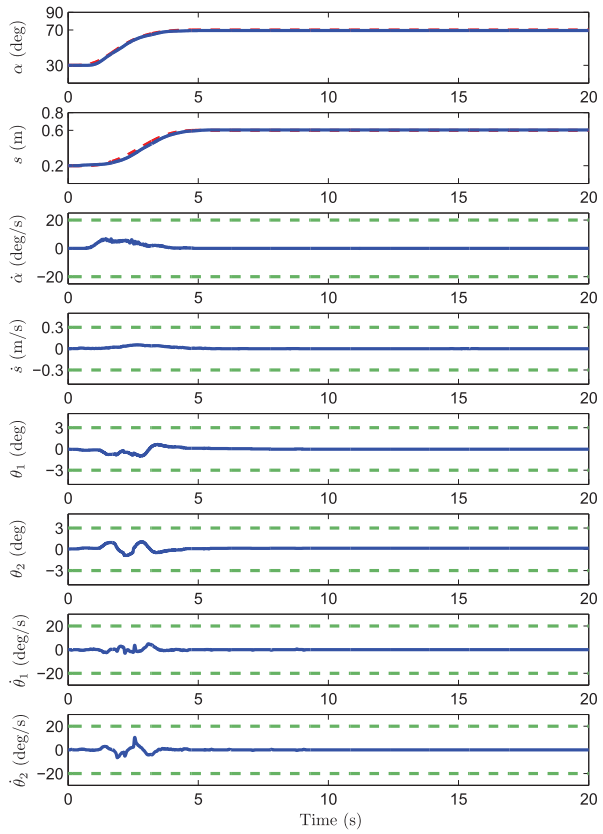

FIGURE 4. Results for Experiment 1: The proposed trajectory planning method (blue solid lines: Experimental results; red dashed lines: Reference trajectories; green dashed lines: Performance constraints).

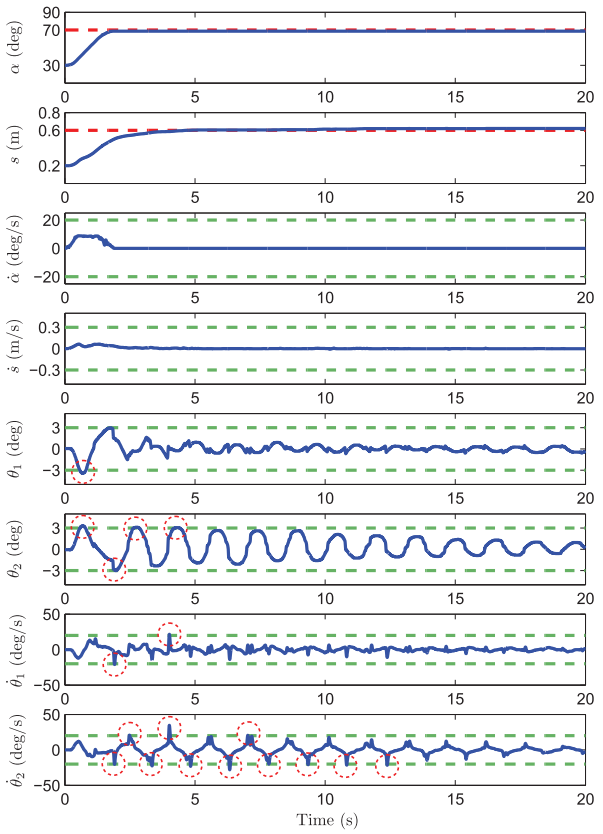

FIGURE 5. Results for Experiment 1: LQR method (blue solid lines: Experimental results; red dashed lines: Desired positions; green dashed lines: Performance constraints).

TABLE 1. Parameters in experiment 1.

Parameter	Physical meaning	Value
m	payload mass	1 kg
l	rope length	0.55 m
α_{r0}	jib initial position	30 deg
α_r	jib desired position	70 deg
s_{r0}	trolley initial position	0.2 m
s_r	trolley desired position	0.6 m
$v_{\alpha\,\max}$	slew velocity constraint	20 deg/s
$a_{\alpha\,\max}$	slew acceleration constraint	30 deg/s^2
$\theta_{k\,\max}$	swing amplitude constraints	3 deg
$v_{\theta_{k\,\max}}$	swing velocity constraints	20 deg/s
$v_{i\,\max}$	velocity constraints of auxiliary signals	0.3 m/s
$a_{i\,\max}$	acceleration constraints of auxiliary signals	0.3 m/s^2
$j_{i\,\max}$	jerk constraints of auxiliary signals	0.3 m/s^3

$k = 1,\ 2, i = 1,\ 2,\ 3.$

state constraints are set in TABLE 1. Then, according to (27) and Algorithm 1, we can obtain the reference trajectories for the jib and trolley, with $T^* = 5.5170$ s. It takes about 28.6125 s to compute the reference trajectories in MATLAB R2014a in the Windows 10 (64b) operating system (Intel i5-7400 processor, 8 GB memory). In order to track the proposed trajectories, we adopt the traditional PD controller, and the expressions of control inputs are $u_1 = k_{p1}(\alpha^* - \alpha) + k_{d1}(\dot{\alpha}^* - \dot{\alpha})$ and $u_2 = k_{p2}(s^* - s) + k_{d2}(\dot{s}^* - \dot{s})$, where α^* and s^* are the reference trajectories for the jib and trolley, respectively, which can be obtained by (31) and (32). Additionally, the control gains are selected as $k_{p1} = 870$, $k_{d1} = 51$, $k_{p2} = 950$, and $k_{d2} = 72$, respectively.

For the LQR method, two decoupled linear subsystems can be obtained after linearizing the tower crane dynamics. The LQR controllers for the jib slew and trolley translation subsystem are set as $F_j = -k_1(\alpha - \alpha_r) - k_2\dot{\alpha} - k_3\theta_2 - k_4\dot{\theta}_2$ and $F_t = -k_5(s - s_r) - k_6\dot{s} - k_7\theta_1 - k_8\dot{\theta}_1$, respectively. To obtain the appropriate control gains, the cost function of LQR method is chosen as $J = \int_0^\infty \left(\zeta^T Q\zeta + RF^2\right) \mathrm{d}t$, where $\zeta = [\alpha(t) - \alpha_r \quad \dot{\alpha}(t) \quad \theta_2(t) \quad \dot{\theta}_2(t)]^T$ and $\zeta = [s(t) - s_r \quad \dot{s}(t) \quad \theta_1(t) \quad \dot{\theta}_1(t)]^T$ for the jib slew and trolley translation subsystem, respectively. By MATLAB calculation, we can obtain the control gains and the LQR controllers as $u_1 = -38.0058(\alpha - \alpha_r) - 55.2720\dot{\alpha} + 112.3530\theta_2 + 6.4018\dot{\theta}_2$ and $u_2 = -40.3113(s - s_r) - 47.9433\dot{s} + 109.8338\theta_1 + 8.8918\dot{\theta}_1$.

The experimental results for the proposed method are shown in FIGURE 4. It is seen that the jib and trolley can track the reference trajectories accurately; meanwhile, the payload swing is effectively eliminated during the transportation time T^* with almost *zero* residual swing. Furthermore, all state variables and their velocities are restricted in the suitable ranges (green dashed lines in FIGURE 4). Specifically, with velocities ($\dot{\alpha}$ and $\dot{s}$) and accelerations ($\ddot{\alpha}$ and $\ddot{s}$) of the jib and trolley being constrained appropriately, the control inputs are accordingly limited as well. In addition, the payload swing

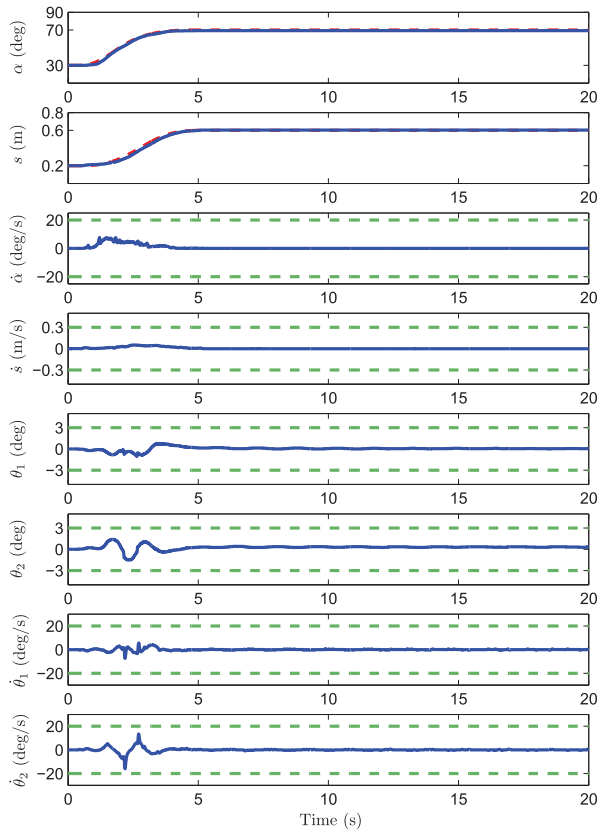

FIGURE 6. Results for Experiment 2-Case 1: The proposed trajectory planning method with changed payload mass (blue solid lines: Experimental results; red dashed lines: Reference trajectories; green dashed lines: Performance constraints).

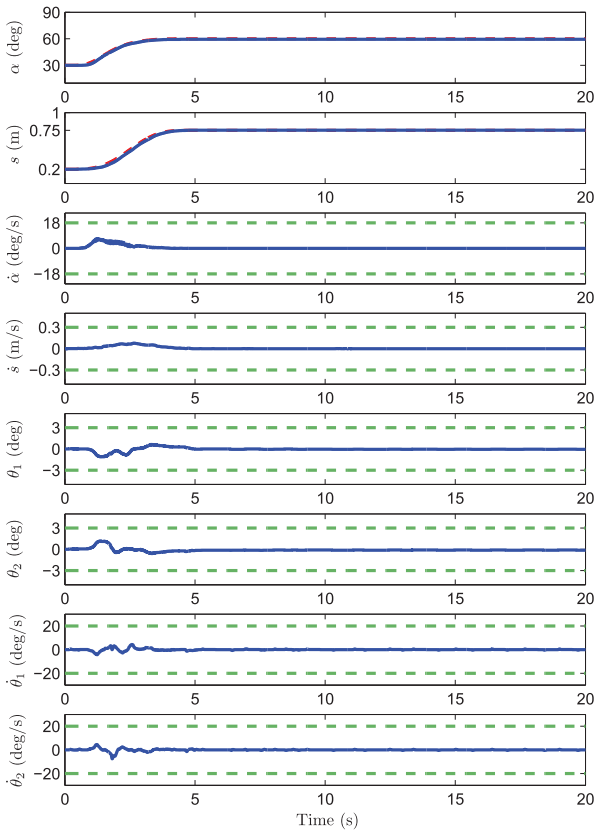

FIGURE 7. Results for Experiment 2-Case 2: The proposed trajectory planning method with changed rope length and different desired positions (blue solid lines: Experimental results; red dashed lines: Reference trajectories; green dashed lines: Performance constraints).

angles (θ_1 and θ_2) are limited within 3 deg and angular velocities ($\dot{\theta}_1$ and $\dot{\theta}_2$) also satisfy the physical constraints, which ensure the control performance of the unactuated states of tower crane systems.

As shown in FIGURE 5, controlled by the LQR method, the jib and trolley can also arrive at the desired positions (red dashed lines in FIGURE 5) at about 5 s; however, the control performance of payload swing suppression is inferior than the proposed method especially for θ_2. More concretely, as the red dotted circles labeled, the payload swing angles (θ_1 and θ_2) and their angular velocities ($\dot{\theta}_1$ and $\dot{\theta}_2$) exceed the specific constraints (green dashed lines in FIGURE 5), which may cause safety risks. In addition, from FIGURE 5, it is clear that there are obvious residual swings by the LQR controller.

2) EXPERIMENT 2

In order to further validate the reliability of the proposed method, we implement experiments by considering the following cases:

- *Case 1: different payload mass.* A 1 kg payload is replaced by a 1.5 kg one, while the initial/desired positions, state constraints, and control gains are still selected the same as those in TABLE 1.
- *Case 2: different desired positions along with a changed rope length.* The rope length is changed from 0.55 m to 0.45 m while the desired positions are changed to $\alpha = 60$ deg and $s = 0.75$ m. According to the real application, we change the angular velocity constraint as $v_{\alpha\,\max} = 18$ deg/s while the other constraints remain the same as those in TABLE 1. It takes 27.1895 s to obtain the reference trajectories and T^* is calculated as 4.9757 s.

The experimental results are depicted in FIGURE 6 and FIGURE 7, respectively. According to (32), we find that the designed trajectories will not change with different payload masses. Comparing FIGURE 6 and FIGURE 4, it is clear that all the curves are similar, and the control performance is not influenced by different masses. In Case 2, although the rope length and the desired positions are changed, the control performance is still satisfactory. As shown in FIGURE 7, the jib and trolley arrive at the desired positions fast and accurately with effective swing elimination, and all the physical constraints are satisfied, indicating that the proposed method can be used under different working requirements.

V. CONCLUSION

This paper proposes a new time-(sub)optimal trajectory planning method with state constraints for 4-DOF tower crane systems. From the theoretical viewpoint, in the trajectory planning process, the physical constraints of state variables

together with their velocities and accelerations are fully into consideration assisted by the auxiliary signals, which theoretically ensures the satisfactory transient performance during a shortest possible transportation time. On the practical side, two group of hardware experiments verify that by tracking the reference trajectories, the jib and trolley can reach the desired positions accurately with rapid payload elimination under different working requirements; moreover, all the state variables can be restricted well within the specific ranges.

ACKNOWLEDGMENT

Zhuoqing Liu and Tong Yang contributed equally to this paper.

REFERENCES

[1] N. Sun, Y. Wu, H. Chen, and Y. Fang, "Antiswing cargo transportation of underactuated tower crane systems by a nonlinear controller embedded with an integral term," *IEEE Trans. Autom. Sci. Eng.*, to be published. doi: 10.1109/TASE.2018.2889434.

[2] H. Ouyang, X. Deng, H. Xi, J. Hu, G. Zhang, and L. Mei, "Novel robust controller design for load sway reduction in double-pendulum overhead cranes," *Proc. Inst. Mech. Eng., C, J. Mech. Eng. Sci.*, to be published. doi: 10.1177/0954406218813383.

[3] M. N. Abourraja *et al.*, "A multi-agent based simulation model for rail–rail transshipment: An engineering approach for gantry crane scheduling," *IEEE Access*, vol. 5, pp. 13142–13156, 2017.

[4] O. Sawodny, H. Aschemann, and S. Lahres, "An automated gantry crane as a large workspace robot," *Control Eng. Pract.*, vol. 10, no. 12, pp. 1323–1338, Dec. 2002.

[5] J. Huang, E. Maleki, and W. Singhose, "Dynamics and swing control of mobile boom cranes subject to wind disturbances," *IET Control Theory Appl.*, vol. 7, no. 9, pp. 1187–1195, Jun. 2013.

[6] N. Uchiyama, "Robust control of rotary crane by partial-state feedback with integrator," *Mechatronics*, vol. 19, no. 8, pp. 1294–1302, Dec. 2009.

[7] N. Sun, T. Yang, H. Chen, Y. Fang, and Y. Qian, "Adaptive anti-swing and positioning control for 4-DOF rotary cranes subject to uncertain/unknown parameters with hardware experiments," *IEEE Trans. Syst., Man, Cybern. Syst.*, to be published. doi: 10.1109/TSMC.2017.2765183.

[8] G. Bartolini, A. Pisano, and E. Usai, "Second-order sliding-mode control of container cranes," *Automatica*, vol. 38, no. 10, pp. 1783–1790, Oct. 2002.

[9] M. F. Daqaq and Z. N. Masoud, "Nonlinear input-shaping controller for quay-side container cranes," *Nonlinear Dyn.*, vol. 45, nos. 1–2, pp. 149–170, Jul. 2006.

[10] Q. H. Ngo and K. S. Hong, "Sliding-mode antisway control of an offshore container crane," *IEEE/ASME Trans. Mechtronics*, vol. 17, no. 2, pp. 201–209, Apr. 2012.

[11] G. Tang, C. Shi, Y. Wang, and X. Hu, "Strength analysis of the main structural component in ship-to-shore cranes under dynamic load," *IEEE Access*, vol. 7, pp. 23959–23966, 2019.

[12] X. Li and Z. Geng, "A novel trajectory planning-based adaptive control method for 3-D overhead cranes," *Int. J. Syst. Sci.*, vol. 49, no. 16, pp. 3332–3345, Oct. 2018.

[13] W. He, Y. Ouyang, and J. Hong, "Vibration control of a flexible robotic manipulator in the presence of input deadzone," *IEEE Trans. Ind. Informat.*, vol. 13, no. 1, pp. 48–59, Feb. 2017.

[14] X. Xin and Y. Liu, "Reduced-order stable controllers for two-link underactuated planar robots," *Automatica*, vol. 49, no. 7, pp. 2176–2183, Jul. 2013.

[15] M. H. Korayem, H. Tourajizadeh, and M. Bamdad, "Dynamic load carrying capacity of flexible cable suspended robot: Robust feedback linearization control approach," *J. Intell. Robot. Syst.*, vol. 60, nos. 3–4, pp. 341–363, Dec. 2010.

[16] S. Yang, Z. Li, R. Cui, and B. Xu, "Neural network-based motion control of an underactuated wheeled inverted pendulum model," *IEEE Trans. Neural Netw. Learn. Syst.*, vol. 25, no. 11, pp. 2004–2016, Nov. 2014.

[17] J.-X. Xu, Z.-Q. Guo, and T. H. Tong, "Design and implementation of integral sliding-mode control on an underactuated two-wheeled mobile robot," *IEEE Trans. Ind. Electron.*, vol. 61, no. 7, pp. 3671–3681, Jul. 2014.

[18] Y. Wu, N. Sun, Y. Fang, and D. Liang, "An increased nonlinear coupling motion controller for underactuated multi-TORA systems: Theoretical design and hardware experimentation," *IEEE Trans. Syst., Man, Cybern. Syst.*, to be published. doi: 10.1109/TSMC.2017.2723478.

[19] W. Sun, S.-F. Su, J. Xia, and V.-T. Nguyen, "Adaptive fuzzy tracking control of flexible-joint robots with full-state constraints," *IEEE Trans. Syst., Man, Cybern. Syst.*., to be published. doi: 10.1109/TSMC.2018.2870642.

[20] D. Verscheure, B. Demeulenaere, J. Swevers, J. De Schutter, and M. Diehl, "Time-optimal path tracking for robots: A convex optimization approach," *IEEE Trans. Autom. Control*, vol. 54, no. 10, pp. 2318–2327, Oct. 2009.

[21] N. Sun, Y. Wu, X. Liang, and Y. Fang, "Nonlinear stable transportation control for double-pendulum shipboard cranes with ship-motion-induced disturbances," *IEEE Trans. Ind. Electron.*, to be published. doi: 10.1109/TIE.2019.2893855.

[22] J. Davila, L. Fridman, and A. Levant, "Second-order sliding-mode observer for mechanical systems," *IEEE Trans. Autom. Control*, vol. 50, no. 11, pp. 1785–1789, Nov. 2005.

[23] T. Vyhlídal, M. Anderle, J. Bušek, and S. I. Niculescu, "Time-delay algorithms for damping oscillations of suspended payload by adjusting the cable length," *IEEE/ASME Trans. Mechatronics*, vol. 22, no. 5, pp. 2319–2329, Oct. 2017.

[24] X. Lai, P. Zhang, Y. Wang, and M. Wu, "Position-posture control of a planar four-link underactuated manipulator based on genetic algorithm," *IEEE Trans. Ind. Electron.*, vol. 64, no. 6, pp. 4781–4791, Jun. 2017.

[25] N. Sun, Y. Fang, H. Chen, Y. Fu, and B. Lu, "Nonlinear stabilizing control for ship-mounted cranes with ship roll and heave movements: Design, analysis, and experiments," *IEEE Trans. Syst., Man, Cybern. Syst.*, vol. 48, no. 10, pp. 1781–1793, Oct. 2018.

[26] Y. Li and Q. Xu, "Adaptive sliding mode control with perturbation estimation and PID sliding surface for motion tracking of a piezo-driven micromanipulator," *IEEE Trans. Control Syst. Technol.*, vol. 18, no. 4, pp. 798–810, Jul. 2010.

[27] F. Padula and A. Visioli, "Inversion-based feedforward and reference signal design for fractional constrained control systems," *Automatica*, vol. 50, no. 8, pp. 2169–2178, 2014.

[28] K. L. Sorensen and W. E. Singhose, "Command-induced vibration analysis using input shaping principles," *Automatica*, vol. 44, no. 9, pp. 2392–2397, 2008.

[29] M. J. Maghsoudi, Z. Mohamed, S. Sudin, S. Buyamin, H. I. Jaafar, and S. M. Ahmadc, "An improved input shaping design for an efficient sway control of a nonlinear 3D overhead crane with friction," *Mech. Syst. Signal Process.*, vol. 92, pp. 364–378, Aug. 2017.

[30] W. Blajer and K. Kolodziejczyk, "Motion planning and control of gantry cranes in cluttered work environment," *IET Control Theory Appl.*, vol. 1, no. 5, pp. 1370–1379, Sep. 2007.

[31] N. Sun, Y. Fang, Y. Zhang, and B. Ma, "A novel kinematic coupling-based trajectory planning method for overhead cranes," *IEEE/ASME Trans. Mechatronics*, vol. 17, no. 1, pp. 166–173, Feb. 2012.

[32] Z. Wu and X. H. Xia, "Optimal motion planning for overhead cranes," *IET Control Theory Appl.*, vol. 8, no. 17, pp. 1833–1842, 2014.

[33] M. Zhang, X. Ma, H. Chai, X. Rong, X. Tian, and Y. Li, "A novel online motion planning method for double-pendulum overhead cranes," *Nonlinear Dyn.*, vol. 85, no. 2, pp. 1079–1090, 2016.

[34] G. Boschetti, R. Caracciolo, D. Richiedei, and A. Trevisani, "Moving the suspended load of an overhead crane along a pre-specified path: A non-time based approach," *Robot. Comput.-Integr. Manuf.*, vol. 30, no. 3, pp. 256–264, Jun. 2014.

[35] D. Chwa, "Sliding-mode-control-based robust finite-time antisway tracking control of 3-D overhead cranes," *IEEE Trans. Ind. Electron.*, vol. 64, no. 8, pp. 6775–6784, Aug. 2017.

[36] H. Lee, Y. Liang, and D. Segura, "A sliding-mode antiswing trajectory control for overhead cranes with high-speed load hoisting," *ASME J. Dyn. Syst., Meas., Control*, vol. 128, no. 4, pp. 842–845, 2006.

[37] N. Sun, T. Yang, Y. Fang, Y. Wu, and H. Chen, "Transportation control of double-pendulum cranes with a nonlinear quasi-PID scheme: Design and experiments," *IEEE Trans. Syst., Man, Cybern. Syst.*, to be published. doi: 10.1109/TSMC.2018.2871627.

[38] X. Wu and X. He, "Nonlinear energy-based regulation control of three-dimensional overhead cranes," *IEEE Trans. Autom. Sci. Eng.*, vol. 14, no. 2, pp. 1297–1308, Apr. 2017.

[39] N. Sun, Y. Wu, H. Chen, and Y. Fang, "An energy-optimal solution for transportation control of cranes with double pendulum dynamics: Design and experiments," *Mech. Syst. Signal Process.*, vol. 102, pp. 87–101, Mar. 2018.
[40] R. Banavar, F. Kazi, R. Ortega, and N. S. Manjarekar, "The IDA-PBC methodology applied to a gantry crane," in *Proc. Math. Theory Netw. Syst.*, Jul. 2006, pp. 143–147.
[41] N. Sun, Y. Wu, Y. Fang, and H. Chen, "Nonlinear antiswing control for crane systems with double-pendulum swing effects and uncertain parameters: Design and experiments," *IEEE Trans. Autom. Sci. Eng.*, vol. 15, no. 3, pp. 1413–1422, Jul. 2018.
[42] J. H. Yang and S. H. Shen, "Novel approach for adaptive tracking control of a 3-D overhead crane system," *J. Intell. Robotic Syst.*, vol. 62, no. 1, pp. 59–80, 2011.
[43] D. Liu, J. Yi, D. Zhao, and W. Wang, "Adaptive sliding mode fuzzy control for a two-dimensional overhead crane," *Mechatronics*, vol. 15, no. 5, pp. 505–522, 2005.
[44] W. Yu, M. A. Moreno-Armendariz, and F. O. Rodriguez, "Stable adaptive compensation with fuzzy CMAC for an overhead crane," *Inf. Sci.*, vol. 181, no. 21, pp. 4895–4907, Nov. 2011.
[45] D. Qian, S. Tong, and S. Lee, "Fuzzy-Logic-based control of payloads subjected to double-pendulum motion in overhead cranes," *Automat. Construct.*, vol. 65, pp. 133–143, May 2016.
[46] Y. Zhao and H. Gao, "Fuzzy-model-based control of an overhead crane with input delay and actuator saturation," *IEEE Trans. Fuzzy Syst.*, vol. 20, no. 1, pp. 181–186, Feb. 2012.
[47] M. I. Solihin, Wahyudi, and A. Legowo, "Fuzzy-tuned PID anti-swing control of automatic gantry crane," *J. Vib. Control*, vol. 16, no. 1, pp. 127–145, 2010.
[48] L.-H. Lee, P.-H. Huang, Y.-C. Shih, T.-C. Chiang, and C.-Y. Chang, "Parallel neural network combined with sliding mode control in overhead crane control system," *J. Vib. Control*, vol. 20, no. 5, pp. 749–760, Apr. 2012.
[49] Z. Sun, Y. Bi, X. Zhao, Z. Sun, C. Ying, and S. Tan, "Type-2 fuzzy sliding mode anti-swing controller design and optimization for overhead crane," *IEEE Access*, vol. 6, pp. 51931–51938, 2018.
[50] F. Ju, Y. S. Choo, and F. S. Cui, "Dynamic response of tower crane induced by the pendulum motion of the payload," *Int. J. Solids Struct.*, vol. 43, no. 2, pp. 376–389, 2006.
[51] H. M. Omar and A. H. Nayfeh, "Gain scheduling feedback control of tower cranes with friction compensation," *J. Vib. Control*, vol. 10, no. 2, pp. 269–289, 2004.
[52] D. Blackburn *et al.*, "Command shaping for nonlinear crane dynamics," *J. Vib. Control*, vol. 16, no. 4, pp. 477–501, Apr. 2010.
[53] D. Blackburn, J. Lawrence, J. Danielson, W. Singhose, T. Kamoi, and A. Taura, "Radial-motion assisted command shapers for nonlinear tower crane rotational slewing," *Control Eng. Pract.*, vol. 18, no. 5, pp. 523–531, 2010.
[54] M. Böck and A. Kugi, "Real-time nonlinear model predictive path-following control of a laboratory tower crane," *IEEE Trans. Control Syst. Technol.*, vol. 22, no. 4, pp. 1461–1473, Jul. 2014.
[55] N. Sun, Y. Fang, H. Chen, B. Lu, and Y. Fu, "Slew/translation positioning and swing suppression for 4-DOF tower cranes with parametric uncertainties: Design and hardware experimentation," *IEEE Trans. Ind. Electron.*, vol. 63, no. 10, pp. 6407–6418, Oct. 2016.
[56] A. T. Le and S.-G. Lee, "3D cooperative control of tower cranes using robust adaptive techniques," *J. Franklin Inst.*, vol. 354, no. 18, pp. 8333–8357, 2017.
[57] S. C. Duong, E. Uezato, H. Kinjo, and T. Yamamoto, "A hybrid evolutionary algorithm for recurrent neural network control of a three-dimensional tower crane," *Automat. Construct.*, vol. 23, pp. 55–63, May 2012.
[58] J. Matuško, Š. Ileš, F. Kolonic, and V. Lešic, "Control of 3D tower crane based on tensor product model transformation with neural friction compensation," *Asian J. Control*, vol. 17, no. 2, pp. 443–458, Mar. 2015.
[59] T.-S. Wu, M. Karkoub, W.-S. Yu, C.-T. Chen, M.-G. Her, and K.-W. Wu, "Anti-sway tracking control of tower cranes with delayed uncertainty using a robust adaptive fuzzy control," *Fuzzy Sets Syst.*, vol. 290, pp. 118–137, May 2016.
[60] V. Mahout, "Path planning for non linear systems using trigonometric splines," *IFAC Proc. Volumes*, Prague, Czech, vol. 38, no. 1, pp. 954–959, 2005.

ZHUOQING LIU received the B.S. degree in intelligent science and technology from Nankai University, Tianjin, China, in 2019, where she is currently pursuing the M.S. degree with the Institute of Robotics and Automatic Information Systems under the supervision of Dr. N. Sun.

Her research interest includes the nonlinear control of underactuated systems including tower cranes.

TONG YANG received the B.S. degree in automation from Nankai University, Tianjin, China, in 2017, where she is currently pursuing the Ph.D. degree in control science and engineering with the Institute of Robotics and Automatic Information Systems under the supervision of Dr. N. Sun.

Her research interests include the nonlinear control of underactuated systems, including rotary cranes, offshore cranes, and tower cranes.

NING SUN (S'12–M'14) received the B.S. degree (Hons.) in measurement and control technology and instruments from Wuhan University, Wuhan, China, in 2009, and the Ph.D. degree (Hons.) in control theory and control engineering from Nankai University, Tianjin, China, in 2014.

He is currently an Associate Professor with the Institute of Robotics and Automatic Information Systems, Nankai University. His research interests include underactuated systems (e.g., cranes) and nonlinear control with applications to mechatronic systems.

Dr. Sun is an Organizing/Program Committee Member for several international conferences. He received the First Class Prize of the Natural Science Award from the Chinese Association for Artificial Intelligence (CAAI), in 2017, the First Class Prize of the Tianjin Natural Science Award, in 2018, the Golden Patent Award of Tianjin, in 2017, the *International Journal of Control, Automation, and Systems* (IJCAS) Academic Activity Award, in 2018, the Outstanding Ph.D. Dissertation Award from the Chinese Association of Automation (CAA), in 2016, the Best Application Paper Award from the 31st Youth Academic Annual Conference of CAA, in 2016, and the Nomination Award of the Guan Zhao-Zhi Best Paper Award at the 32nd Chinese Control Conference, in 2013. He received the Japan Society for the Promotion of Science (JSPS) Postdoctoral Fellowship for Research in Japan (Standard). He is the Executive Editor of *Measurement and Control* and serves as an Associate Editor (Editorial Board Member) for several journals, including the IEEE Access, the IJCAS, the *International Journal of Precision Engineering and Manufacturing*, the *International Journal of Advanced Robotic Systems*, *Information Technology and Control*, and *Advances in Mechanical Engineering*.

YONGCHUN FANG (S'00–M'02–SM'08) received the B.S. and M.S. degrees in control theory and applications from Zhejiang University, Hangzhou, China, in 1996 and 1999, respectively, and the Ph.D. degree in electrical engineering from Clemson University, Clemson, SC, USA, in 2002.

From 2002 to 2003, he was a Postdoctoral Fellow with the Sibley School of Mechanical and Aerospace Engineering, Cornell University, Ithaca, NY, USA. He is currently a Professor with the Institute of Robotics and Automatic Information Systems, Nankai University, Tianjin, China. His research interests include nonlinear control, visual servoing, control of underactuated systems, and AFM-based nanosystems.

Dr. Fang is a Distinguished Professor of the Cheung Kong Scholars Program and received the National Science Fund for Distinguished Young Scholars of China. He was an Associate Editor for the *ASME Journal of Dynamic Systems, Measurement, and Control*.